A Deep Graph Cut Model for 3D Brain Tumor Segmentation

Arijit De, Mona Tiwari, Enrico Grisan and Ananda S. Chowdhury

Abstract— **Brain tumor segmentation plays a key role in tumor diagnosis and surgical planning. In this paper, we propose a solution to the 3D brain tumor segmentation problem using deep learning and graph cut from the MRI data. In particular, the probability maps of a voxel to belong to the object (tumor) and background classes from the UNet are used to improve the energy function of the graph cut. We derive new expressions for the data term, the region term and the weight factor balancing the data term and the region term for individual voxels in our proposed model. We validate the performance of our model on the publicly available BRATS 2018 dataset. Our segmentation accuracy with a dice similarity score of 0.92 is found to be higher than that of the graph cut and the UNet applied in isolation as well as over a number of state of the art approaches.**

I. INTRODUCTION

Formation of abnormal groups of cells inside or near the brain leads to brain tumor. These abnormal cells disrupt normal brain functions thereby leading to considerable degradation of the health of a patient.

A challenge faced by the radiologist and the neurosurgeon is to demarcate the tumor margins when the lesion is poorly defined and is diffusely infiltrative. Recently, there have been concerns about the usage of Gadolinium and its deposition in the brain. Neuro-radiologists would prefer a shorter but accurate way of identifying tumors that can speed up the pre-operative diagnosis, maybe by using only a few essential MR sequences. A pre-operative assessment of the tumor using 3D visualization techniques help in planning the surgical path and trajectory. The surgeon can then avoid the eloquent areas, blood vessels and other vital structures during surgery. This leads to excellent outcome for the patient with minimal complications and morbidity.

Classical techniques such as level sets [1] and graph cuts [2] have been extensively used for segmentation [3], where, domain specific image features (e.g. gradient, intensity, texture, etc.) can be combined within an energy minimization framework. However, a majority of these algorithms rely heavily on initialization such as manual seeding, and are susceptible to segmentation errors due to unreliable location

Arijit De and Ananda S. Chowdhury are with the Department of Electronics and Telecommunication Engineering, Jadavpur University, Kolkata 700032 India (e-mail: arijitde.etce.rs@jadavpuruniversity.in; as.chowdhury@jadavpuruniversity.in).

Mona Tiwari is with Department of Neuro-radiology, Institute of Neurosciences, Kolkata, West Bengal 700017, India (e-mail: drmonatiwari@gmail.com).

Enrico Grisan is with Department of Information Engineering, University of Padova, Italy and School of Engineering, London South Bank University, UK

of the initial seed. In recent times, deep convolutional neural networks (CNN) have shown significant improvement, especially, in segmentation and classification problems [4]–[6]. However, traditional fully supervised techniques disregard domain knowledge which could help in better segmentation. 2D CNNs employ 2D convolutional kernels for segmenting a single slice. Although, they are able to leverage contextual information across the height and width of the slice to make predictions, they are unable to extract any information from the adjacent slices. 3D CNNs mitigate this issue by using 3D convolutional kernels to predict 3D segmentation maps for a volumetric patch of a scan. This ability to grasp inter-slice context can improve the segmentation performance [7], [8]. Recently, good segmentation performance have been achieved using a modified 3D CNN known as V-Net using Attention Guided (AG) , Squeeze and Excitation (SE) [9] and multi depth fusion modules [10]. Combination of classical and deep learning techniques have been used in solving many medical imaging problems where data driven and domain specific approaches have been cascaded or ensembles of both techniques have been formed [11], [12]. We took inspiration from [11] where they mixed deep learning and graph cut to segment lung nodules. However, their work was restricted to 2D. They also did not modify the terms in the energy function of the graph cut, which can have significant impact on the segmentation performance. Furthermore, they used manual seeds for initialization of the graph cut algorithm. In sharp contrast, we have addressed the tumor segmentation problem in 3D. The data term, the smoothness term and the parameter which relatively weighs these two terms in the energy function of the graph cut are modified through a 3D deep learned model. We have further removed the need to manually initialize the seeds.

In this paper, we propose a deep graph cut model for segmenting brain tumors in 3D. The proposed approach combines data driven (graph cut) and domain specific (deep learning) strategies that are suitable for addressing the complexities of segmenting highly irregular structures like brain tumor. We term our solution Deep Graph Cut (DGC). DGC embeds deep learned probability maps of object (tumor) and background (everything other than tumor) voxels into the energy function of the graph cut. The deep learned voxel probabilities make the model highly robust to initialization errors. On the other hand, the unsupervised graph cut component can accurately segment structures through an energy minimization framework. To motivate the reader, we include a 3D segmentation result using the proposed method in Fig. 1. In this figure, it is difficult to distinctly identify the tumor region (marked in red circles) in the 2D views, but the full
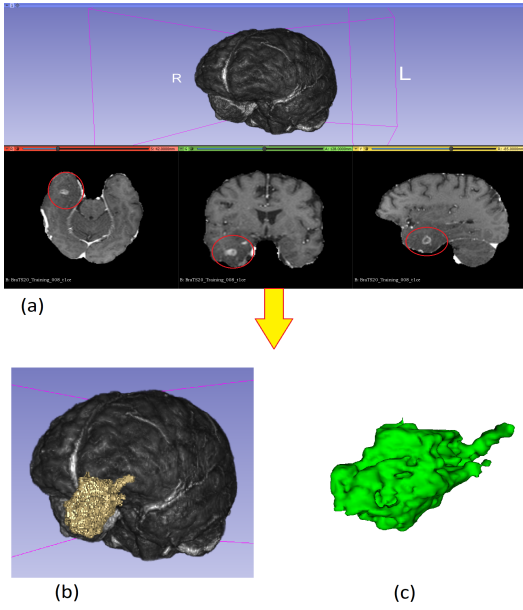
Fig. 1: (a) 2D and 3D views of the input image with the tumor range marked in red circle, (b) Volumetric view of the segmented tumor region inside the brain, (c) 3D view of the segmented tumor only

segmented tumor is shown in 3D inside the brain and in another 3D view containing only the segmented tumor (in green). We now summarize our contributions below:

1) Methodologically speaking, we propose a novel 3D segmentation framework by combining UNet and graph cut. In this framework, we derive new expressions for the data term, the smoothness term and the weighting parameter in the energy function of the graph cut from the probability maps of tumor and non-tumor voxels obtained from the UNet.

2) From the application perspective, we solve 3D tumor segmentation, an important problem in brain imaging which has a far-reaching impact for the radiologists and the neurosurgeons.

II. PROPOSED METHOD

In this section, 3D segmentation using UNet and graph cut are discussed first. We then describe in details our proposed solution (DGC). The section is completed with Algorithm 1 showing the steps of this DGC.

A. 3D Brain Tumor Segmentation using UNet

We choose 3D UNet [13], a fully convolutional deep network architecture as it is efficiently handles pixel-wise semantic labelling. UNet is an encoder-decoder network widely used for medical image segmentation [14]. This deep network can yield decent performance even in the absence of large amount of training data.

B. 3D Brain Tumor Segmentation using Graph Cut

The input MRI is a 3D gray-scale volume which is represented by a 3D weighted graph $G = G(V, E)$. Each voxel x is a vertex in G and the set of all voxels is denoted

by X. We consider two additional nodes, 'source' and 'sink', which are respectively denoted by s and t. We consider two types of edges/links, namely, the t-links (T) and the n-links (N). Each voxel x is connected to s and t via t-links. We use dense 26-neighborhood, denoted by $Ne(x)$ for each voxel x. Let y be a neighbour of x. So, $y \in Ne(x)$ and we connect x and y via a n-link. Thus, $V = X \cup s \cup t$ and $E = T \cup N$. Let us define a segmentation A, which is a voxel-wise classification of all voxels into two classes, i.e., either the "object" or the "background". Hence, following [2], we need to minimize the following energy function:

$$\zeta(A) = B(A) + \lambda R(A) \tag{1}$$

where $B(A)$ denotes the boundary properties/smoothness term and $R(A)$ denotes the regional properties/data term of A. Mathematically, these terms are expressed as:

$$B(A) = \sum_{x \in X, y \in Ne(x)} B_{(x,y)} \tag{2}$$

$$R(A) = \sum_{x \in X} R_x \tag{3}$$

C. 3D Brain Tumor Segmentation using Deep Graph Cut

The learned information from 3D UNet is embedded into the energy function of the 3D graphcut to achieve accurate segmentation. For each image, the 3D probability map is extracted from the last convolutional layer to calculate the probability of any voxel to belong to either tumor or background. In the proposed deep graph cut (DGC) model, we introduce a new data term, a new smoothness term and further combine the proposed data term and smoothness terms using a variable weight factor.

The 3D UNet estimates a regression function which maps each voxel of a 3D input image to a corresponding 3D voxel wise segmentation probability map $\mathcal{P} : \mathbb{R}^3 \to (0, 1)$ which also serves as an automated seed for the graph cut algorithm. The deep learned data term is expressed as follows:

$$R_{DGC}(x)(Obj) = -\ln Pr(x = Obj)_{UN} \tag{4}$$

$$R_{DGC}(x)(Bkg) = -\ln Pr(x = Bkg)_{UN} \tag{5}$$

where the terms $Pr(j = Obj)_{UN}$ and $Pr(j = Bkg)_{UN}$ respectively indicate the probability of any voxel j to belong to the object (tumor) class and the background (anything other than tumor) class obtained from the UNet (UN). Naturally, $\forall j$, we have $Pr(j = Obj)_{UN} + Pr(j = Bkg)_{UN} = 1$.

Brain MRI volumes tend to have low contrast between the tumor region and its surrounding structures thereby making the segmentation process difficult. In order to handle such constraints, we modify the smoothness term. The modification relies on the difference in the probabilities of any voxel and its neighboring voxel to belong to the tumor and the background classes. The improved smoothness term is given by:

$$B_{DGC}(x, y) = K_{(x,y)} \exp{-(\frac{(I_x - I_y)^2}{2\sigma^2})} \times \frac{1}{d(x,y)} \times \frac{1}{\delta(x,y)_{DGC}} \tag{6}$$

where the term $d(x,y)$ denotes the Euclidean distance between two voxels x and y having intensity values I_x and I_y respectively. The term $K_{(x,y)}$ is based on the probabilities of these two voxels (x and y) to have the same segmentation class and is formulated as follows:

$$K_{(x,y)} = 1 - |Pr(x = Obj)_{UN} - Pr(y = Obj)_{UN}| \quad (7)$$

The value of $K_{(x,y)}$ is higher when the probability of two neighboring voxels to belong to the same segmentation class is similar, i.e., when their absolute difference in probability values are less. The factor σ is chosen manually depending on image noise level. The term $\delta(x,y)_{DGC}$ denotes the sum of differences between probabilities of neighbouring voxels x and y to belong to the class tumor (object) and the class background. This can be expressed as:

$$\delta(x,y)_{DGC} = |Pr(x = Obj)_{UN} - Pr(y = Obj)_{UN}|+$$
$$|Pr(x = Bkg)_{UN} - Pr(y = Bkg)_{UN}|$$
$$(8)$$

Note that a low $\delta(x,y)_{UN}$, which is computed from the probability maps in UNet, leads to higher/better smoothness.

In the graph cut-based segmentation framework, the parameter λ regulates the relative importance of the smoothness term and the data term (see Eq. 1). It is crucial to properly choose this parameter as it largely influences the quality of the segmentation [2]. Ideally, the optimal value of λ should neither cause over-segmentation nor under-segmentation. However, finding an optimal value for this parameter remains a challenging problem. To remove the dependence on manual selection of this parameter, we propose in this work an automated calculation of λ, once again from the probability maps obtained from the 3D UNet. The calculation is based on the following careful observations:

1) If a voxel lies deep within the foreground or the background region, more importance should be given to the smoothness term. For such an interior voxel, the surrounding voxels generally have considerably higher probabilities to belong to the same segmentation class.
2) The data term is given more importance whenever a voxel lies nearer to edge or boundary region. For such a terminal voxel, the surrounding voxels usually have much lower probabilities to belong to the same segmentation class.

Hence, we write $\lambda \propto \psi_{UN}(x)$, where $\psi_{UN}(x)$ is given by:

$$\psi_{UN}(x) = |Pr(x = Obj)_{UN} - Pr(x = Bkg)_{UN}| \quad (9)$$

Note that a higher $\psi_{UN}(x)$, which is determined from the probability maps in UNet denotes that the voxel is more towards the interior of object (tumor). Unlike [15], where the authors used classical techniques to modify λ, we employed deep learned probability maps to modify it. Hence, the final form of λ becomes:

$$\lambda_{DGC}(x) = P\psi_{UN}(x) \quad (10)$$

where P is a constant which maps $\psi_{DGC}(x)$ that lies between $[0,1]$ to λ that lies between $[\lambda_{Min}, \lambda_{Max}]$. For our experiments, we have taken $\lambda_{Min} = 1$ and $\lambda_{Max} = 100$. Finally, combining equations (4), (5), (6) and (10), we get the final modified energy function as shown below:

$$\zeta_{DGC}(A) = \sum_{x \in X, y \in Ne(x)} B_{DGC}(x,y)+$$
$$\lambda_{DGC}(x) \sum_{x \in X} R_{DGC}(x)$$
$$(11)$$

Minimizing the above energy function via graph cut according to [2] will result in a 3D segmented image.

Algorithm 1: DGC

Input: Trained 3D UNet model M, 3D voxel grid graph G, where V is the set of nodes/voxels and E is the set of edges

Output: 3D grid graph G_{out} with desired segmentation

1 Compute data term $R_{DGC}(x)$ for each voxel in $x \in G$ using Equations 4 and 5
2 Compute smoothness term $B_{DGC}(x,y)$ for each voxel x and its neighbour $y \in N_e(x)$ in G as shown in Equation 6
3 Compute weight factor λ for each voxel in $x \in G$ using Equation 10
4 Compute the final energy function using Equation 11, perform Graph cut and store the result in G_{out}.
5 **return** G_{out}

III. EXPERIMENTAL RESULTS

In this section, we first discuss data preparation. We then extensively evaluate our solution including ablation studies and comparisons with external approaches. We implemented UNet in Tensorflow [16] and trained it on HP-Z640 workstation with 14 Core Intel Xeon processor, 128GB of memory and NVIDIA Titan RTX 24GB dedicated graphics processor. The network is trained for 500 epochs with stochastic gradient descent with initial learning rate of 0.0001, weight decay of 0.00001 and mini-batch size equal to 2 samples. We have used Adam Optimizer and weighted cross-entropy loss in the process. For the quantitative performance evaluation, Dice Similarity Coefficient (DSC) is employed [17].

A. Data Preparation

For experimentation, publicly available BRATS 2018 dataset [18], [19] is used. It is already split into training, validation and test sets containing 285, 66 and 192 scans respectively. We use only T1-weighted contrast-enhanced (T1CE) sequences from each scan for our experiments as we found T1CE best represents the data in terms of contrast. The data were publicly made available with some pre-processing, i.e. they were co-registered to the same anatomical template, skull-stripped and interpolated to a resolution of $1mm^3$. As all the scans were stored in compressed Nifti image format (i.e. .nii.gz), we used SimpleITK library [20] to convert nifti format images into 3D numpy array [21]. We further normalized all input images to have zero mean and

TABLE I: Ablation study I: Graph cut, Graph Cut enhanced with combinations of (a) DGC data term (b) DGC smoothness term (c) DGC variable weight factor. Best values are shown in **bold**.

Modification	DSC
Graph Cut (Boykov et al. [2])	0.53 ± 0.17
GC with (a) and (b) only	0.883 ± 0.23
GC with (b) and (c) only	0.856 ± 0.19
GC with (a) and (c) only	0.87 ± 0.034
DGC (GC with (a), (b) and (c))	**0.92 ± 0.073**

TABLE II: Ablation study II: Graph Cut, 3D UNet, DL-GC in 2D and DGC. Best values are shown in **bold**.

Algorithm	DSC
Graphcut (Boykov et al. [2])	0.53 ± 0.17
3D UNet (Çiçek et al. [13])	0.83 ± 0.034
DL-GC in 2D (Mukherjee et al. [11])	0.82 ± 0.062
DGC	**0.92 ± 0.073**

unit standard deviation (std) based on non-zero voxels only. For augmentation, we applied a random intensity shift (-0.1 . . . 0.1 of image intensity std) and scale (0.9 . . . 1.1) on the input images. We also applied random horizontal flips (for x axis) with a probability 0.5. As UNet requires the input image with a specific resolution [22], and to reduce the memory constraints while minimizing information loss, we crop each image volume from its original resolution $(240 \times 240 \times 155)$ to a resolution of $(192 \times 192 \times 144)$. As the λ parameter is learned from the UNet, only one parameter (σ) that is used in equation (6), is manually set to 4 during the training phase after various trials.

B. Ablation Studies

We have conducted two ablation studies. The first ablation study is undertaken to demonstrate the individual contributions of the data term, smoothness term and the variable weight factor in the proposed DGC algorithm. The results are shown in Table I. For all the combinations, UNet was used. As is evident from this table, all the three terms contribute towards improving the performance of the DGC algorithm. We also conduct a second ablation study to examine the contributions of the 3D UNet and the Graph Cut used in isolation. Qualitative segmentation outputs for two datasets are illustrated in Fig. 2 and 3. We also implement Mukherjee et al.'s work [11] where they have modified only the data term of Graph cut using 2D UNet and required manual seeding, but we automatically initialized the seed for Graph Cut using [32]. Table II indicates that DGC algorithm clearly outperforms basic 3D UNet [13], vanilla Graph cut [2] and 2D-DLGC algorithm [11].

C. Comparison with State of the art Methods

We now compare our method with other state of the art segmentation approaches in table III. The methods are diverse in nature with some of them using deep learning and others are not. Among the methods which have not employed deep learning, we choose two Graph Cut based methods, one on random walks [24], one method using Competitive Expectation Maximization Algorithm [23] and another using normalization techniques [25]. Among the deep learning based methods, We use a 2D CNN [29], a 3D CNN [26], V-Nets [9], [10] and a ensemble 3D UNet [31]. The results of comparisons in Table III are shown only for whole tumor segmentation with three metrics namely Dice Score, sensitivity and specificity and it clearly establishes the superiority of our approach over all the competing methods. Most of the methods did not show sensitivity and specificity values and hence we have kept it blank for those methods.
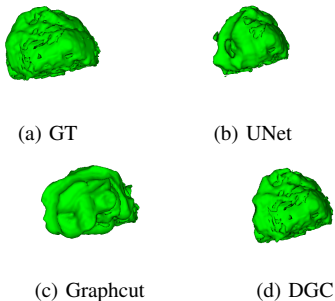

Fig. 2: Qualitative comparisons for one dataset: (a) Ground Truth (GT), (b) Segmentation using 3D UNet (DSC = 0.862), (c) Segmentation using Graph Cut (DSC = 0.812), (d) Segmentation using DGC (DSC = 0.91)
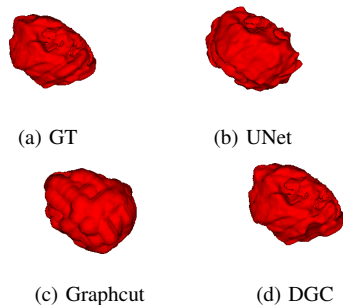

Fig. 3: Qualitative comparisons for a second dataset: (a) Ground Truth (GT), (b) Segmentation using 3D UNet (DSC = 0.877), (c) Segmentation using Graph Cut (DSC = 0.897), (d) Segmentation using DGC (DSC = 0.934).

IV. CONCLUSION

Detection, delineation and characterisation of 3D brain tumors using MR imaging is found to be very important in guiding the treatment strategy. In this paper, we have shown how UNet and graph cut can be combined to achieve better segmentation performance in 3D. New expressions for the constituent terms in the graph cut energy function are explicitly derived with help of the probability maps obtained from the UNet. We have established through comprehensive experimentation that our proposed deep graph cut model yields competitive performance on the publicly available

TABLE III: Comparison of State of the art Methods. Best values are shown in **bold**.

Algorithm	DSC	Sensitivity	Specificity
EM and Graphcut [23]	0.70 ± 0.21	-	-
Random Walks [24]	0.72 ± 0.08	-	-
Normalized Graphcut [25]	0.85	-	-
3D CNN [26]	0.85	0.877	-
SegNet 2D [27]	0.85	-	-
AGSE V-Net [9]	0.85	0.83	0.99
Multi Depth V-Net [10]	0.86	0.958	0.99
MCCNN 2D [28]	0.87	0.87	-
2D Deep Networks [29]	0.88	0.84	0.88
2D M-UNet [30]	0.90	-	-
3D UNet Ensemble [31]	0.90	-	-
DGC	$\mathbf{0.92 \pm 0.073}$	$\mathbf{0.94 \pm 0.003}$	$\mathbf{0.91 \pm 0.008}$

BRATS dataset. In future, we will extend the proposed approach for multi-label tumor segmentation.

REFERENCES

[1] Stanley Osher and Ronald P Fedkiw, "Level set methods: an overview and some recent results," *Journal of Computational Physics*, vol. 169, no. 2, pp. 463–502, 2001.

[2] Yuri Y Boykov and M-P Jolly, "Interactive graph cuts for optimal boundary & region segmentation of objects in nd images," in *ICCV*. IEEE, 2001, vol. 1, pp. 105–112.

[3] Rukhmini Roy, Pranavesh Banerjee, and Ananda S Chowdhury, "A level set based unified framework for pulmonary nodule segmentation," *IEEE Signal Processing Letters*, vol. 27, pp. 1465–1469, 2020.

[4] Yann LeCun, Yoshua Bengio, and Geoffrey Hinton, "Deep learning," *Nature*, vol. 521, no. 7553, pp. 436–444, 2015.

[5] Wenjun Yan, Yuanyuan Wang, Menghua Xia, and Qian Tao, "Edge-guided output adaptor: Highly efficient adaptation module for cross-vendor medical image segmentation," *IEEE Signal Processing Letters*, vol. 26, no. 11, pp. 1593–1597, 2019.

[6] Tianyu Shen, Chao Gou, Jiangong Wang, and Fei-Yue Wang, "Simultaneous segmentation and classification of mass region from mammograms using a mixed-supervision guided deep model," *IEEE Signal Processing Letters*, vol. 27, pp. 196–200, 2020.

[7] Guotai Wang and Wenqi Li et al., "Interactive medical image segmentation using deep learning with image-specific fine tuning," *IEEE Transactions on Medical Imaging*, vol. 37, no. 7, pp. 1562–1573, 2018.

[8] Yan Hu and Yong Xia, "3d deep neural network-based brain tumor segmentation using multimodality magnetic resonance sequences," in *International MICCAI Brainlesion Workshop*. Springer, 2017, pp. 423–434.

[9] Xi Guan, Guang Yang, Jianming Ye, Weiji Yang, Xiaomei Xu, Weiwei Jiang, and Xiaobo Lai, "3d agse-vnet: an automatic brain tumor mri data segmentation framework," *BMC Medical Imaging*, vol. 22, no. 1, pp. 1–18, 2022.

[10] He Huang, Guang Yang, Wenbo Zhang, Xiaomei Xu, Weiji Yang, Weiwei Jiang, and Xiaobo Lai, "A deep multi-task learning framework for brain tumor segmentation," *Frontiers in Oncology*, vol. 11, 2021.

[11] Suvadip Mukherjee, Xiaojie Huang, and Roshni R Bhagalia, "Lung nodule segmentation using deep learned prior based graph cut," in *ISBI*. IEEE, 2017, pp. 1205–1208.

[12] Rukhmini Roy, Tapabrata Chakraborti, and Ananda S Chowdhury, "A deep learning-shape driven level set synergism for pulmonary nodule segmentation," *Pattern Recognition Letters*, vol. 123, pp. 31–38, 2019.

[13] Özgün Çiçek, Ahmed Abdulkadir, Soeren S Lienkamp, Thomas Brox, and Olaf Ronneberger, "3d u-net: learning dense volumetric segmentation from sparse annotation," in *MICCAI*. Springer, 2016, pp. 424–432.

[14] L. Liu, J. Cheng, Q. Quan, F. Wu, Y. Wang, and J. Wang, "A survey on u-shaped networks in medical image segmentations," *Neurocomputing*, vol. 409, pp. 244 – 258, 2020.

[15] Ashish K Rudra, Mainak Sen, Ananda S Chowdhury, Ahmed Elnakib, and Ayman El-Baz, "3d graph cut with new edge weights for cerebral white matter segmentation," *Pattern Recognition Letters*, vol. 32, no. 7, pp. 941–947, 2011.

[16] Martín Abadi and Ashish Agarwal wt al., "TensorFlow: Large-scale machine learning on heterogeneous systems," 2015, Software available from tensorflow.org.

[17] Lee R Dice, "Measures of the amount of ecologic association between species," *Ecology*, vol. 26, no. 3, pp. 297–302, 1945.

[18] Bjoern H. Menze, Andras Jakab, and Stefan Bauer et al., "The multimodal brain tumor image segmentation benchmark (BRATS)," *IEEE Transactions on Medical Imaging*, vol. 34, no. 10, pp. 1993–2024, Oct. 2015.

[19] Spyridon Bakas and Hamed Akbari et al., "Advancing the cancer genome atlas glioma MRI collections with expert segmentation labels and radiomic features," *Scientific Data*, vol. 4, no. 1, Sept. 2017.

[20] Bradley C. Lowekamp, David T. Chen, Luis Ibáñez, and Daniel Blezek, "The design of SimpleITK," *Frontiers in Neuroinformatics*, vol. 7, 2013.

[21] Charles R. Harris and et al., "Array programming with NumPy," *Nature*, vol. 585, no. 7825, pp. 357–362, Sept. 2020.

[22] Olaf Ronneberger, Philipp Fischer, and Thomas Brox, "U-net: Convolutional networks for biomedical image segmentation," in *International Conference on Medical image computing and computer-assisted intervention*. Springer, 2015, pp. 234–241.

[23] Valentina Pedoia, Sergio Balbi, and Elisabetta Binaghi, "Fully automatic brain tumor segmentation by using competitive em and graph cut," in *ICIAP*. Springer, 2015, pp. 568–578.

[24] Leo Grady, Thomas Schiwietz, Shmuel Aharon, and Rüdiger Westermann, "Random walks for interactive organ segmentation in two and three dimensions: Implementation and validation," in *MICCAI*. Springer, 2005, pp. 773–780.

[25] S Sasikanth and S Suresh Kumar, "Glioma tumor detection in brain mri image using anfis-based normalized graph cut approach," *International Journal of Imaging Systems and Technology*, vol. 28, no. 1, pp. 64–71, 2018.

[26] Konstantinos Kamnitsas et al., "Efficient multi-scale 3d cnn with fully connected crf for accurate brain lesion segmentation," *Medical Image Analysis*, vol. 36, pp. 61–78, 2017.

[27] Salma Alqazzaz, Xianfang Sun, Xin Yang, and Len Nokes, "Automated brain tumor segmentation on multi-modal mr image using segnet," *Computational Visual Media*, vol. 5, no. 2, pp. 209–219, 2019.

[28] Kai Hu, Qinghai Gan, Yuan Zhang, Shuhua Deng, Fen Xiao, Wei Huang, Chunhong Cao, and Xieping Gao, "Brain tumor segmentation using multi-cascaded convolutional neural networks and conditional random field," *IEEE Access*, vol. 7, pp. 92615–92629, 2019.

[29] Mohammad Havaei and Axel Davy et al., "Brain tumor segmentation with deep neural networks," *Medical Image Analysis*, vol. 35, pp. 18–31, 2017.

[30] H. Zhao, Y. Guo, and Y. Zheng, "A compound neural network for brain tumor segmentation," in *ICIP*, 2019, pp. 1435–1439.

[31] Li Sun, Songtao Zhang, Hang Chen, and Lin Luo, "Brain tumor segmentation and survival prediction using multimodal mri scans with deep learning," *Frontiers in Neuroscience*, vol. 13, pp. 810, 2019.

[32] Paul Bourke, "Calculating the area and centroid of a polygon," *Swinburne Univ. of Technology*, vol. 7, 1988.